東北大学機関リポジトリ
TOUR
Tohoku University Repository

# Damage of twisted tape tethers on debris collision



| | |
|---|---|
| 著者 | Yoshiyuki Uwamino, Michihiro Fujiwara, Honoka Tomizaki, Kiyonobu Ohtani, Kanjuro Makihara |
| journal or publication title | International Journal of Impact Engineering |
| volume | 137 |
| page range | 103440 |
| year | 2020-03 |
| URL | http://hdl.handle.net/10097/00134676 |



doi: 10.1016/j.ijimpeng.2019.103440

Creative Commons : 表示 - 非営利 - 改変禁止
http://creativecommons.org/licenses/by-nc-nd/3.0/deed.ja

This is the accepted version of the following article:

Uwamino, Y., Fujiwara, M., Tomizaki, H., Ohtani, K., and Makihara, K.,
"Damage of Twisted Tape Tethers on Debris Collision," *International Journal of Impact Engineering*, Vol. 137, 2020, Article No. 103440. (DOI: 10.1016/j.ijimpeng.2019.103440).

# Damage of Twisted Tape Tethers on Debris Collision

Yoshiyuki UWAMINO[a], Michihiro FUJIWARA[a], Honoka TOMIZAKI[a], Kiyonobu OHTANI[b], and Kanjuro MAKIHARA[*,a]

[a] Department of Aerospace Engineering, Tohoku University, 6-6-01 Aramaki-Aza-Aoba, Aoba-Ward, Sendai 980-8579, Japan

[b] Institute of Fluid Science, Tohoku University, 2-2-1 Katahira, Aoba-Ward, Sendai 980-8577, Japan

## Abstract

The amount of space debris will increase in the future because of collisions with other debris, even if no future space launches are carried out. Therefore, debris removal is essential for sustainable space development. The electrodynamic tether system is a promising method to remove debris because it does not require any propellants; however, it can be severed by a collision with a small piece of debris. As a tape tether is wider and thinner than a conventional solid cylindrical tether, it may overcome this drawback. The tape tether, however, can be twisted and transformed to a non-ideal shape. This paper considers a scenario in which the tape tether is twisted to create a loop shape. Every impact generates a debris cloud, which may subsequently impact another part of the tether that happens to be located in the direction the debris cloud is emitted to. This could cause a cascade effect where a single impact results in multiple collisions that lead to significant damage of the tether. Through hypervelocity impact experiments, collisions on the loop part are evaluated to gain new insights into the loop phenomenon of the tape tether system. Based on the experimental results, the rate of severance of the tape tether was compared with that of the conventional solid cylindrical tether. When only a small part of the tape tether is in loops, the rate of severance of the tape tethers is much lower than that of the conventional solid cylindrical tethers. Hence, tape tethers have a considerable advantage over conventional tethers when the looped range is narrow.

**Keywords:** Tape Tether, Debris Removal, Space Debris, Electrodynamic Tether, Hypervelocity Impact

## Nomenclature

$a$: Damaged length of a tape tether in the lateral direction [mm]
$b$: Damaged length of a tape tether in the circumferential direction [mm]
$d$: Diameter of the projectile or debris [mm]
$d_m$: Minimum diameter of debris that may sever a tether [mm]
$F(d)$: Cumulative flow rate of debris as a function of $d$ [1/mm$^2$/year]
FoS: Factor of safety [-]
$L_D$: Damaged length [mm]
$L_{DC}$: Critical damaged length [mm]
$L_T$: Total length of a tether [mm]
$r$ : Radius of a loop [mm]
$R$: Rate of severance [1/year]
$S_{eff}$: Effective collision area [mm$^2$]
$v_p$: Velocity of a projectile [km/s]

* Corresponding author. *E-mail address:* makihara@ssl.mech.tohoku.ac.jp

$w$: Width of a tape tether [mm]
$\gamma$ : Loop ratio [-]
$\theta$: Impact angle against the surface of a tape tether [°]

**Suffixes**

LOOP: Loop shaped part of a tape tether
FLT: Flat shaped part of a tape tether
SCT: Solid cylindrical tether
TPT: Tape tether consisting of loop and flat shaped parts

# 1. Introduction

## 1.1. Background on Space Debris

Space debris is an urgent issue to be addressed for sustainable space development. Space debris, such as non-functional spacecraft and fragments from satellite breakups, consists of artificial objects that are useless in the present or future. Space debris in low Earth orbits (LEOs) travel at very high speeds (7-8 km/s), and even small debris particles can release a significant amount of kinetic energy upon impact. Space debris hinders space development because impacts of space debris particles onto spacecraft can lead to functional degradation up to mission loss. There are so many pieces of space debris in LEO that the amount of space debris will increase due to collision events even if no future launches are carried out [1,2]. Therefore, it is critical to remove space debris, especially from the LEOs, to be able to safely continue space activities.

Several systems of active debris removal (ADR) have been proposed to mitigate the number of large debris objects in LEO. Most ADR systems slow down their target, lower their orbit, and initiate earlier reentry to remove the debris [1-3]. ADR systems based on conventional propulsion systems with rocket engines have high launch costs because of the mass of the propellant. An electrodynamic tether (EDT) system is a promising method because it does not need any propellants. The EDT system consists of an electrically conductive tether and an emitter. Figure 1 shows an image of the EDT system. First, the conductive tether is attached to a removal target and deployed toward the Earth. Then, the emitter starts to emit electrons from the bottom end of the tether while the tether collects electrons from the space plasma around the Earth. Because of the motion of these electrons, an electric circuit that consists of the tether, emitter, and space plasma is generated. Thus, electric current flows in the longitudinal direction along the tether. The tether consequently generates a Lorentz force owing to the interference between the current flow and the geomagnetic field. The removal target is slowed down by this force because the force acts in the direction opposite to that of the target's movement. The reduced velocity of the satellite causes the orbital altitude of the satellite to decrease. As the EDT system does not require any propellant to deorbit the removal target, the total mass of the EDT systems can be much smaller than that of a conventional rocket-based de-orbit system. The small mass of the EDT system is a great advantage over conventional ADR systems [4-14]. Aluminum is generally expected to be used as the material of EDTs because it has good conductivity and small weight.

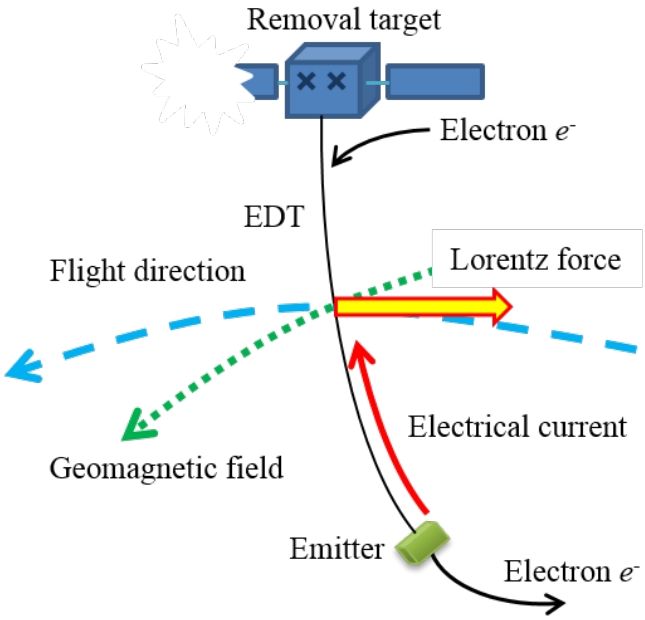


**Fig. 1.** Schematic of EDT system.

A drawback of the EDT is that it can be severed by a collision with even a small piece of debris because of its thin shape. The severance of the tether leads to a failure of ADR missions. Thus, severance has to be avoided. Several shapes have been proposed to increase the robustness of the tether against these collisions. The most basic shape of the EDT is a solid cylinder, which is made of a columnar metallic wire. Sanmartin et al. [4] calculated the electrical current flowing along a bare tether based on orbital motion limited theory. Hayashida and Robinson [5] and Pardini et al. [6] reported that solid cylindrical tethers can be severed as a result of collisions with small pieces of debris. It was reported that the severance probability is more accurate when we consider the fact that the fracture area of the tether is larger than the path area of the debris [7]. Here, the path area refers to the projected area with the same dimensions as a debris particle, whereas the fracture area is the resultant damaged area that is expanded by high-temperature melt. Experimental results indicate that the fracture area will increase after the collision of the tether with a piece of space debris owing to high temperature and stress. Kawamoto et al. [8] proposed a net tether, which is made of braided wires of aluminum and stainless steel, and demonstrated through hypervelocity impact (HVI) experiments that they are more robust against the debris impacts than solid cylindrical tethers. Makihara and Matsumoto [9] proposed hollow cylindrical tethers that have larger diameters when compared to solid cylindrical tethers with the same linear density. Tethers with larger diameters may be more robust against the collisions with small pieces of debris. They estimated the survivability of hollow cylindrical tethers (probability that the EDTs finish the ADR missions without being severed) based on the results of the HVI experiments and numerical simulations. They reported that the survivability of hollow cylindrical tethers is higher than that of solid cylindrical tethers. A tether with a wide and thin shape has also been proposed and is referred to as a tape tether in these studies [10-14]. Francesconi et al. [10] developed ballistic limit equations for tape tethers from experiments and numerical simulations. This study assumes that the tape tethers always remain an ideal flat shape when determining the size of the holes in tape tethers generated by the collisions with debris. Khan et al. [11] defined a criterion of the severance of tape tethers based on the data of Francesconi et al. [10] and estimated the probability of severance during ADR missions as $< 0.006$ year$^{-1}$ km$^{-1}$ when the tape tether has a width of 45 mm and a thickness of 50 μm, which results in a cross-sectional area of 2.3 mm$^2$. Makihara and Kondo [12] evaluated the advantage of tape tethers and their superior geometries from two perspectives: the stress concentration around the damaged holes generated by the debris impacts and the numbers of the electrons collected by the tethers. Fujii et al. [13] studied methods to expand the tape tethers and proposed to fold the tape tether for storage and expand it in outer space. They succeeded in expanding 300 m of a tape tether at an altitude of 300 km with a sounding rocket [14].

Figure 2 shows an image of the motion of the EDTs. One end of the EDT is attached to the removal target and the other end is attached to the emitter. The EDTs may be twisted easily because there is no structure to maintain the shape while the removal targets and the emitters rotate.

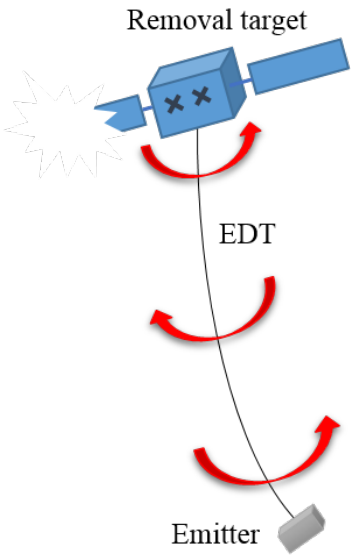


**Fig. 2.** Schematic of EDT that is twisted in ADR mission.

Figure 3 shows the shapes that appear when thin and wide objects such as tape tethers are twisted [15]. In Fig. 3g, the horizontal axis $T$ is non-dimensional tension, and the vertical axis $\theta$ is the normalized twist angle, where $T \equiv$ tensile force / (Young's modulus × thickness × width), $\theta \equiv$ twist angle × width / length. Figure 3g shows the phase diagram of the shapes observed when $T$ and $\theta$ are applied, as illustrated in Fig. 3a, on the tape tether that has a length of $L = 450$ mm, a width of 25.4 mm, and a thickness of 0.127 mm. Figures 3b–f show shapes typically observed. The shape of the twisted tape tethers is categorized into six groups. The loop illustrated as the central part of Fig. 3f is a curved surface that wraps a rod with an elliptic cross-section. In this paper, a collision between the loop and debris is described. When the debris impacts the loop, a part of debris and the loop fragment or melt and spread like a cloud leaving a hole in this side of the loop. This cloud is called a debris cloud [16, 17]. The debris cloud impacts the other side of the loop and further damages the tether. As the debris cloud spreads wider than the original diameter of the debris, the damage due to the debris cloud is larger than that due to the debris. Thus, the damage on the tape tether with an ideal flat shape is significantly different from the damage on the tethers that are twisted and transformed to loops. The debris impact against the geometries except the loop can be modeled by the debris impact against the flat shaped tape tethers. Moreover, there are papers that have described failure assessments for flat shaped tape tethers [10, 11]. Francesconi et al. [10] and Khan et al. [11] described failure assessments for geometries of the tape tethers other than the loop. This study focuses on the collision of the debris cloud with the tape tether and on the assessment of loop geometry.

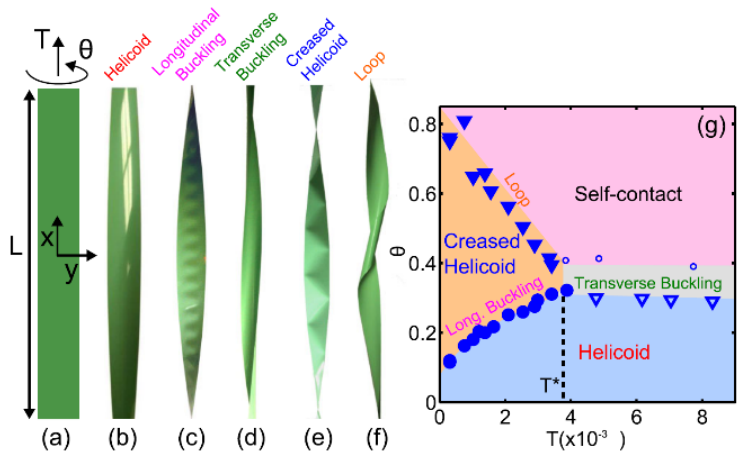


**Fig. 3.** Shapes of twisted tape tether [15].

## 1.2. Research Objectives

The overall objective of this study is to evaluate the practicability of tape tethers when they are twisted and transformed to the loop shape. The specific objectives can be listed as follows:

(1) To understand the damage at the loop generated by debris collision through HVI experiments. Targets with shapes imitating loops are impacted by projectiles (mock space debris) in HVI experiments. The characteristics of the damage of the loops are analyzed by varying the loop radius. In addition, the damage size in the lateral direction is measured. The changes in the damage of the tape tethers depending on their shapes are evaluated quantitatively by comparing the measured size with that from previous reports assuming that the tape tethers always maintain a flat shape.

(2) To estimate the rate of severance of tape tethers in the case that they are twisted and transformed to the loop shapes. The minimum diameter of a debris particle that may sever the tape tether is derived from the results of the HVI experiments. The rate of severance is estimated based on this minimum diameter. The changes in the rate of severance depending on the shapes are evaluated quantitatively by comparing the rate of severance with that calculated assuming that the tether remains flat. In addition, the advantage of the tape tethers is evaluated quantitatively by comparing the rate of severance with that of the conventional solid cylindrical tethers.

In this paper, it will be demonstrated that tape tethers have stronger tolerance against collisions than conventional solid cylindrical tethers and have significant feasibility even when the tape tether is twisted and transformed to a non-ideal shape (i.e., a loop shape).

## 1.3. Size and Material of Tether in This Study

The analysis in this study depends on the tether parameters. The following assumptions are made:

- The diameter of the projectile is sufficiently smaller than the width of the tape tether, to define the hole generated by the collision.
- The diameter of the projectile is sufficiently larger than the thickness of the tape tether, to define the penetrated hole.

The same cross-sectional area and material are considered as in study [11]. The parameters used in this study are as follows:

- Conventional solid cylindrical tether made from aluminum with a diameter of 1.7 mm.

- Tape tether made from aluminum with a width of 7.5 mm, and a thickness of 0.30 mm.

These parameters were set to make the cross-sectional areas equal (2.3 $mm^2$). The two types of tethers have an equal linear density ($6.1 \times 10^{-3}$ g/mm) because they are made of the same material (aluminum, A1050, $2.7 \times 10^{-3}$ $g/mm^3$). This means that the two types of tethers have comparable masses. Because these parameters are set equal to those of the expected tape tether in the study [11], the results of the present work are applicable to actual tether construction.

## 2. Methods of HVI Experiments and Rate of Severance Calculation

### 2.1. Methods and Materials of Hypervelocity Impact Experiments

To conduct the experiments imitating the collisions between tape tethers and space debris, two experimental facilities were used; the two-stage light gas gun (Fig. 4) owned by Institute of Space and Astronautical Science/Japan Aerospace Exploration Agency (ISAS/JAXA) and the single-stage powder gun (Fig. 5) owned by Institute of Fluid Science (IFS) in Tohoku University. The launch tubes are shown on the left of the photos, the experimental chamber on the right. The targets were placed in the experimental chamber and were impacted by the projectiles. A high-speed camera HPV-X (Shimadzu Corporation) was used to photograph the impacts. To capture high-quality and well-lit photographs, flash lamps were placed on the opposite side of the chamber.

**Fig. 4.** Two-stage light gas gun owned by ISAS/JAXA.

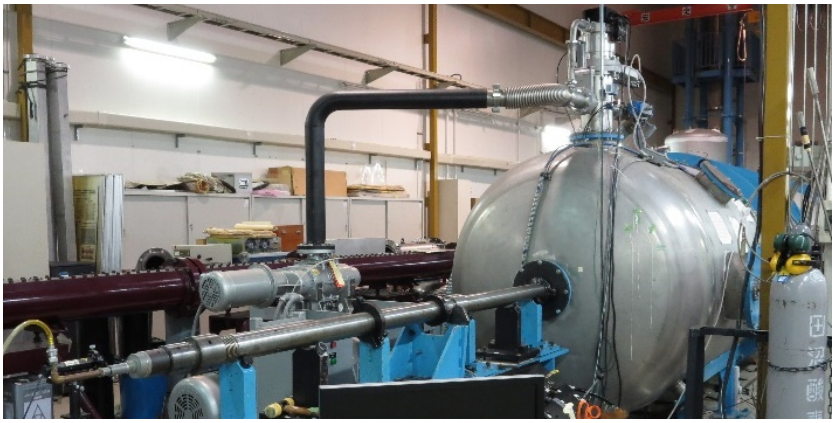

**Fig. 5.** Single-stage powder gun owned by IFS/Tohoku University.

The shape of the loops appears to be similar to a curved surface that wraps a cylinder. In the experiments, cylindrical targets were used to imitate the loop part of the tape tethers. Figure 6 shows the loop on a tape

tether generated by twisting as well as the cylindrical target used in the experiments. The targets were made by cutting aluminum plates (0.3 mm thickness) into rectangles and quasi-statically rolling them up into cylinders. The junction of the cylinder was connected with an adhesive tape. The targets were placed on jigs so that the junction is at the bottom. The projectiles are aluminum spheres (A5052) with a diameter of 3.18 mm and a mass of 45.1 mg. The tension in the tether increases the amount of damage that results in complete failure of the tether because of the stress concentration. During debris removal missions, the tape tether may be under tension from the gravity gradient between the removal target and the emitter or from unstable behavior such as swinging or rotation [18, 19]. The probability of small pieces of debris colliding with the tether while it is under tension may be low, because we assume that both phenomena (i.e., collision and tension) occur only occasionally and for short periods. Therefore, the experiments were carried out without applying tension on the tether.

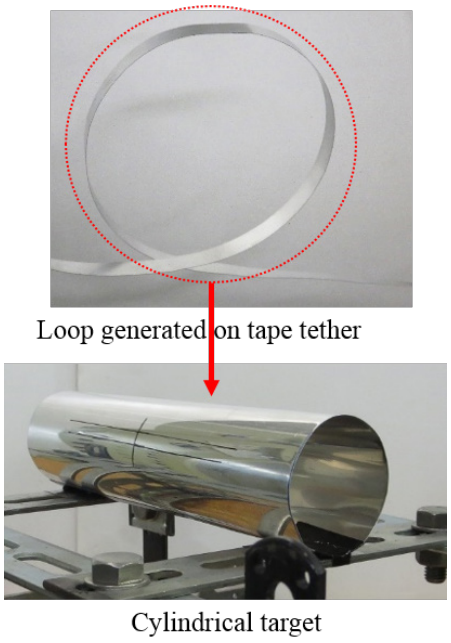


**Fig. 6.** Loop generated on tape tether (above) and cylindrical target imitating loop (bottom).

Figure 7 shows Cartesian coordinates of the HVI experiments. The $x$ axis is set parallel to the trajectory of the projectiles, and the $z$ axis is set in the vertical direction. The center line of the cylinder aligns with the y axis. The impact angle at the impact point is presented as

$$\phi_{\mathrm{p}} = \arcsin\left(z_{\mathrm{p}} / r\right) \tag{1}$$

where $r$ and $z_{\mathrm{p}}$ represent the radius of the targets and the coordinate of the $z$ axis at the impact point, respectively. The experimental cases are summarized in Table 1. To investigate the relationship between the target radius $r$ and the damage of the target, five targets that have different $r$ values were used. The impact velocity was approximately 7 km/s and the impact position (represented as $z_{\mathrm{p}}/r$) was approximately 0.5.

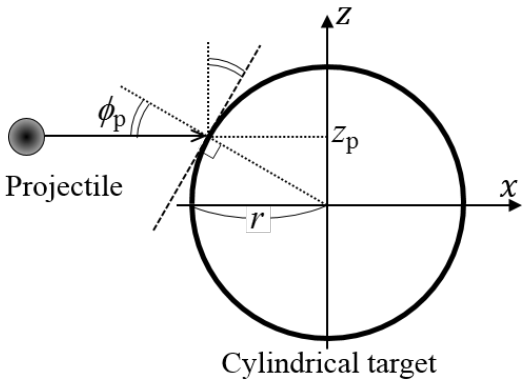


**Fig. 7.** Coordinates of HVI experiment.

**Table 1.** Conditions of HVI experiments.

| Experiment number | 1 | 2 | 3 | 4 | 5 |
|---|---|---|---|---|---|
| Target radius $r$ [mm] | 15 | 25 | 30 | 50 | 100 |
| Impact velocity $v_p$ [km/s] | 6.8 | 6.9 | 7.0 | 6.8 | 6.8 |
| Impact position $z_p$ / $r$ [-] | 0.60 | 0.52 | 0.47 | 0.51 | 0.47 |
| Impact angle $\phi_p$ [°] | 37 | 31 | 28 | 31 | 28 |

## 2.2. Rate of Severance Calculation

### 2.2.1. Outline of Rate of Severance

When an EDT of length $L_T$ (i.e., any kind of long tether) flies in an Earth orbit, the number of impacts that fatally sever an EDT per year is defined as the rate of severance, $R$. The unit of the rate of severance is 1 year$^{-1}$. The risks of being severed for different types of EDTs are compared with the values of the rate of severance. Based on studies [11, 20], the rate of severance of the EDTs is represented as

$$R = -\int_{d_m}^{\infty} S_{eff} \frac{dF(d)}{dd} dd = S_{eff} F(d_m) + \int_{d_m}^{\infty} \frac{dS_{eff}}{dd} F(d) dd \quad (2)$$

where $d_m$ is the minimum diameter of the debris that may sever a tether, $S_{eff}$ is the effective collision area, and $F(d)$ is the cumulative flow rate of debris [6,7,11,20]. Only $d_m$ and $S_{eff}$ are changed for different types of EDTs. In other words, the rate of severance of the tape tether can be obtained by setting $d_m$ and $S_{eff}$. These two factors are discussed in Section 3.3. The calculation of the rate of severance of the ideal flat-shaped tape and solid cylindrical tethers is based on works [11, 20].

### 2.2.2. Impact Angle

It is assumed that all debris fly toward the tethers in the plane of 0° in the local elevation angle. This corresponds to all debris being presumed to fly in the $xy$ plane of Fig. 8. In this figure, the model of the collision between the looped tape tether and the debris is depicted. The $z$ axis is placed on the longitudinal direction of the tether and the $y$ axis is placed on the axis of the loop. According to ORDEM 3.0 [21], the debris flux is concentrated in the range of –5° to 5° in the local elevation angle on the orbit that is used in this paper, see Section 3.4. The debris cloud generated by the collision between the tape tether and the debris certainly impacts the tether again when the impact angle is $\theta = 0°$. In this study, the impact angle $\theta$ is set as 0° to express the most dangerous case, which is a modeling assumption. The impact angle that causes the second collision of the debris cloud with the tape tether is not large. Therefore, the modeling assumption of $\theta = 0°$ causes an overestimation of the risk. In other words, this modeling assumption can

strictly evaluate the tether to a safer side. If the overestimated rate of severance of the tape tether is smaller than that of the conventional solid cylindrical tether, the practicability of the tape tether is regarded as high. The variation in the total length of the tape tether due to the generation of the loop is neglected because the size of the expected loop is considerably smaller than the full length of the tether. Second, the rate of severance of the flat-shaped tape tether is defined as $R_{\mathrm{FLT}}$. In this case, the debris trajectory is supposed to be distributed equally in terms of $\theta$.

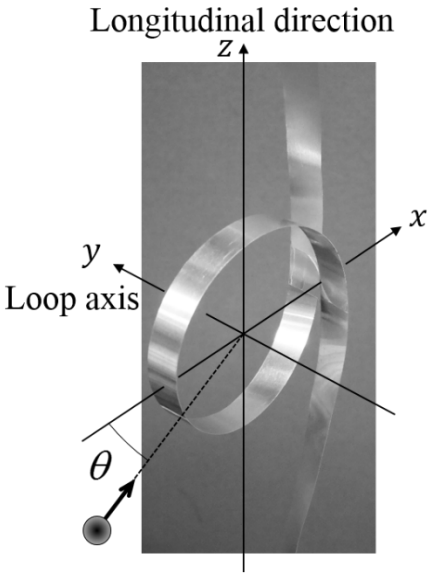


**Fig. 8.** Model of collision between tape tether and debris.

### 2.2.3. Criterion of Severance

The tape tethers are supposed to be severed when they are damaged more than the width of $L_{\mathrm{DC\_TPT}}$. The severance criteria are chosen with factor of safety, referring to studies [7, 9]. First, aluminum is generally expected to be used as the material of the tethers because it has good conductivity and small weight. Because aluminum is expected as the tether material, the material property values are uniquely defined. Therefore, the severance criteria are set to be independent from the material property. Second, the severance criteria are defined only geometrically. The damaged length is regarded to be longer than $L_{\mathrm{DC\_TPT}}$ as the severed part. For this reason, the tension applied to the tether does not appear in the equation for the severance criteria. $L_{\mathrm{DC\_TPT}}$ is defined as

$$L_{\mathrm{DC\_TPT}} \equiv \left(1-1/\mathrm{FoS}\right) w \tag{3}$$

where FoS is the factor of safety and $w$ is the width of the tape tether. In aerospace engineering, the FoS value is commonly set within the range 1.15–1.5. In this study, it is set as FoS = 1.25. The $d_{\mathrm{m}}$ value is the minimum diameter of debris that may sever a tether, and $d_{\mathrm{m}}$ for the loop is represented as $d_{\mathrm{m\_LOOP}}$. The value of $d_{\mathrm{m}}$ is obtained from the experiments, see Section 3.4 below.

### 2.2.4. Shape Mixture Ratio of Loop and Plate

It is supposed that a tape tether has loop parts and flat parts. A part of the tether (length of $L_{\mathrm{LOOP}}$) is transformed into the loop while the other parts always remain flat. The loop ratio $\gamma$ is defined as

$$\gamma \equiv L_{\mathrm{LOOP}} / L_{\mathrm{T}} \tag{4}$$

The severance of tape tethers should be equally evaluated, independent of the severed position in the longitudinal direction, because even if the severed position is near the upper or bottom end of the tether, the tether is disconnected from the emitter and loses its function. Therefore, the rate of severance of the full-length tape tether is represented as

$$R_{\mathrm{TPT}} = \gamma R_{\mathrm{LOOP}} + (1-\gamma) R_{\mathrm{FLT}} \tag{5}$$

In this study, two cases are considered: A case in which the loops are generated in a narrow range ($\gamma$ = 0.002) and another case in which the loops are generated in a considerably wide range ($\gamma$ = 0.1). The value of loop radius is fixed at $r$ = 15–100 mm for the rate of severance calculation. The total length of the tether is typically expected to be 1–10 km [7, 8, 12, 20]. In the calculation, it was fixed at 10 km.

## 3. Results and Discussion of HVI Experiments and Rate of Severance Calculation

### 3.1. Experimental Results

Figure 9 shows the target with $r$ = 15 mm after the HVI experiment. Positions on the targets are identified using the coordinate system shown in Fig. 7. A part of the target in the positive-$x$ region was considerably damaged. The small hole in the negative-$x$ region was created by the impact of the projectile. When this small hole was created, at the same moment, a part of the target and projectile was fragmented or melted, and a lump of debris cloud was generated. The large hole in the positive-$x$ region was created by the impact of the debris cloud. Because the debris cloud spread wider than the original diameter of the projectile, the hole in the positive-$x$ region was large. A part of the target in the negative-$z$ region was deformed inside-out. Because the edge of the deformed part was sharp, it was inferred that this deformed part was not scattered, but rather it was deformed by tearing and rolling when the debris cloud impacted the target.

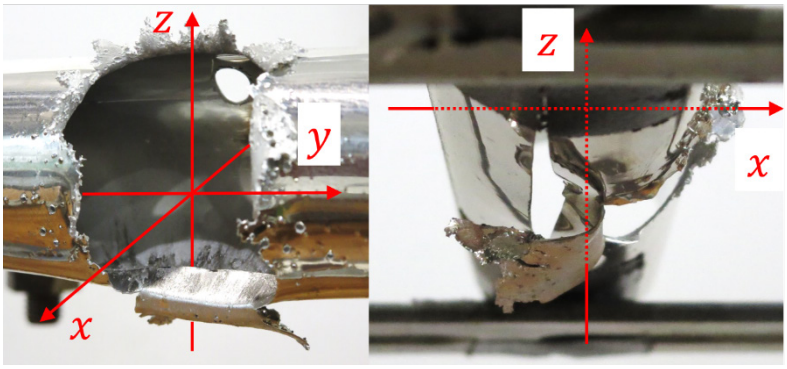


**Fig. 9.** Target with $r$ = 15 mm (left: taken from positive-$x$ region, right: taken from negative-$y$ region).

Figure 10 shows the target with $r$ = 25 mm after the HVI experiment. The cylindrical target was extended into a flat shape, and the inside surface of the target was photographed. The lateral direction of the tape tether (loop axis direction) is the vertical direction in the figure. The holes illustrated as black dots are categorized into three groups: (1) the hole created by the impact of the projectile (Hole 1), (2) the largest of the holes created by the impact of the debris cloud (Hole 2), (3) the holes created by the impact of the debris cloud excluding Hole 2.

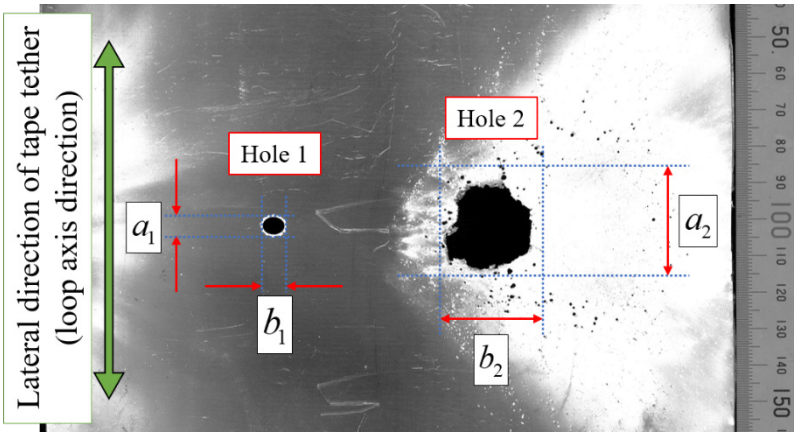


**Fig. 10.** Damage lengths of target after experiment ($r$ = 25 mm).

To evaluate the experimental results quantitatively, the damaged length was defined. There are many small holes around Hole 2; some of them were connected to each other with cracks. When cracks are generated on tape tethers, the range of the successive cracks should be considered severed. Therefore, the damaged length is the maximum extent of holes connected by cracks. Four types of damaged length were measured; $a_1$ and $a_2$ are the damaged lengths in the lateral direction (loop axis direction) of Holes 1 and 2, and $b_1$ and $b_2$ are the damaged lengths in the circumferential direction, respectively. Figure 11 shows the measurement results of $a_1$, $b_1$, $a_2$, and $b_2$. This paper only focuses on the damaged lengths $a_1$ and $a_2$ because the damage in the lateral direction mainly contributes to the severance of tape tethers. From Fig. 11, it can be seen that $a_1$ is almost constant and independent of the change in $r$. Because the impact angle $\phi_p$ was constant (approximately 30°), five experiments can be regarded as identical by considering the phenomenon around the impact points, as the collisions between oblique plates and projectiles. Therefore, it is assumed that the damaged length $a_1$ was almost constant.

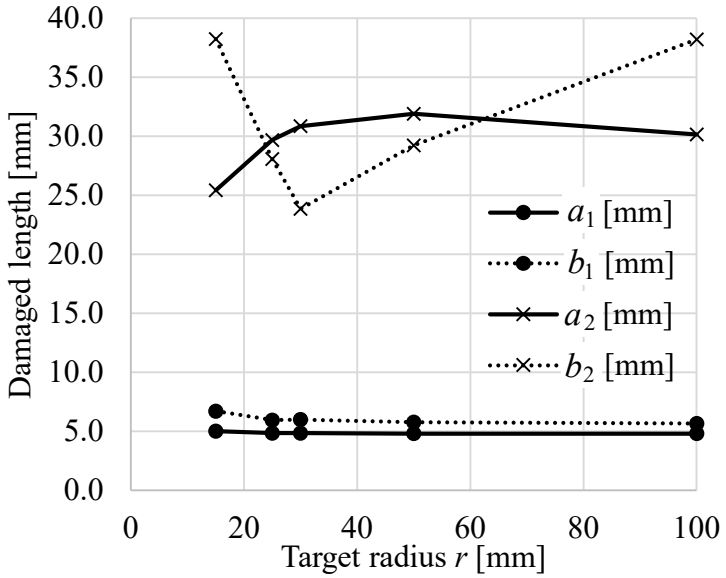


**Fig. 11.** Measurement results of damaged length.

The $a_2$ value monotonically increases when $r \leq 50$ mm and monotonically decreases when $r \geq 50$ mm. These trends are supposed to be due to the spread of the debris cloud. The closer a part of the debris cloud is to the trajectory of the projectile, the higher density of that part is. When $r$ = 15 mm, the distance between the impact point of the projectile and the impact point of the debris cloud was short. Hence, the debris cloud did not spread widely and $a_2$ was small. When $r$ = 50 mm, the distance between the two impact

points was long. Thus, the debris cloud spread widely and $a_2$ was large. When $r$ = 100 mm, the distance between the two impact points was much longer. In this case, the debris cloud spread too much, and the density of the debris cloud became low. Thus, only the center part of the debris cloud damaged the positive side of the target; thus, $a_2$ when $r$ = 100 mm was smaller than that when $r$ = 50 mm.

When the debris impacts the flat-shaped tape tether surface at an angle of $\theta$, an almost perfectly elliptical hole is generated [10]. The length of the major axis of the elliptical hole represents the damage of the flat tape tether in the lateral direction because the major axis is along the lateral direction of the tether. The length of the major axis is named $L_{\mathrm{D\_FLT}}$ to distinguish it from the damaged length of the loop (i.e., $a_1$ and $a_2$). $L_{\mathrm{D\_FLT}}$ can be calculated using the following equation [10]:

$$L_{\mathrm{D\_FLT}} = \begin{cases} k_1 \left( \dfrac{d}{\cos\theta} \right)^{k_2} v_{\mathrm{p}}{}^{k_3} & \text{if } d \le w\cos\theta \\ k_1 w^{k_2} v_{\mathrm{p}}{}^{k_3} & \text{if } d > w\cos\theta \\ 0 & \text{if } v_{\mathrm{p}}\cos\theta < 1 \text{ km/s} \end{cases} \tag{6}$$

where $k_1$, $k_2$, and $k_3$ are constants ($k_1$ = 0.91, $k_2$ = 0.89, $k_3$ = 0.20). According to Eq. (6), $L_{\mathrm{D\_FLT}}$ takes the maximum value at $\theta$ = 80° and the minimum value at $\theta$ = 0° under the same conditions of the HVI experiments in this study ($d$ = 3.2 mm, $v_{\mathrm{p}}$ = 7.0 km/s).

The maximum and minimum values of the damaged length $a_2$ and $L_{\mathrm{D\_FLT}}$ are summarized in Table 2. The maximum of $L_{\mathrm{D\_FLT}}$ is 15.9 mm. However, $a_2$ is at least 25.4 mm. At $\theta$ = 0°, $L_{\mathrm{D\_FLT}}$ = 5.1 mm, whereas $a_2$ = 31.9 mm at the maximum, which is six time larger. Therefore, the lateral damage to the tether is larger in loop shaped parts than in flat parts. Hence, when the tape tethers are twisted and the loops appear, they are more likely to be severed by debris collisions than when they maintain their ideal flat shape.

**Table 2.** Maximum and minimum values of damaged length in lateral direction of tape tether.

| Damaged length | Shape of tape | Minimum value | Maximum value |
|---|---|---|---|
| $a_2$ | Loop ($\theta$ = 0°) | 25.4 mm ($r$ = 15 mm) | 31.9 mm ($r$ = 50 mm) |
| $L_{\mathrm{D\_FLT}}$ | Flat ($r$ = ∞) | 5.1 mm ($\theta$ = 0°) | 15.9 mm ($\theta$ = 80°) |

### 3.2. Normalized Damaged Length

In Fig. 11, the relationship between the damaged lengths of the tape tether in the lateral direction is always $a_2 > a_1$, and the second impact by the debris cloud is the main characteristic phenomenon of the collisions between the debris and the loops. Therefore, $a_2$ represents the damage of the loop in the lateral direction. In Fig. 12, $a_2/d$ is plotted against $r$, where $a_2$ is the damaged length tape tethers in the lateral direction obtained from the HVI experiments. The following quadratic function is chosen as the approximate curve that represents the features of Fig. 12. The value of the coefficient of determination ($R^2$) is 0.874.

$$f_{\mathrm{LOOP}}(r) \equiv a_2 / d = -8.78\times10^{-4} r^2 + 1.15\times10^{-1} r + 6.72 \tag{7}$$

Because debris with diameter $d > d_{\mathrm{m\_LOOP}}$ is necessary to damage the loop with a radius $r > L_{\mathrm{DC\_TPT}}$, the following relationship is derived:

$$d_{\mathrm{m\_LOOP}}(r) = L_{\mathrm{DC\_TPT}} / f_{\mathrm{LOOP}}(r) \tag{8}$$

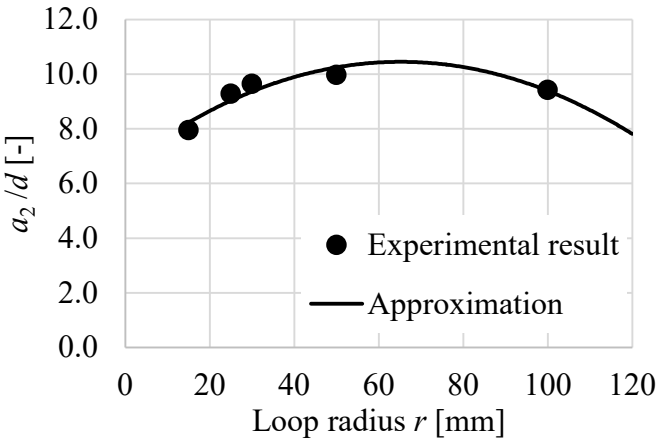


**Fig. 12.** Normalized damaged length of tape tethers obtained from HVI experiments.

### 3.3. Effective Collision Area

To define the effective collision area, $S_{\text{eff}}$, it is supposed that a tape tether is severed if and only if a debris particle with a diameter larger than $d_{\text{m}}$ impacts within the $S_{\text{eff}}$. The effective collision area of the loop is referred to as $S_{\text{eff\_LOOP}}$. It is assumed that the loop is severed only if debris with a diameter larger than $d_{\text{m\_LOOP}}$ impacts the inside of the effective collision area $S_{\text{eff\_LOOP}}$. Figure 13 shows the schematic of the damage of the tape tethers for $d \geq d_{\text{m\_LOOP}}$. The value of $S_{\text{eff\_LOOP}}$ is calculated geometrically in Fig. 13. At the same time, $a_2$ is the damaged width generated by the debris cloud if the width of the tether is infinite, and its value is derived from Eq. (7). The boundary of the debris cloud can be captured with image-extraction methods [22]. Only the area overlapped with $a_2$ is damaged because the tether width is finite. The damaged width reaches $L_{\text{DC\_TPT}}$ when

$$2 \times \frac{a_2}{2} = \left( y_{\text{impact}} + \frac{a_2}{2} - \frac{w}{2} \right) + L_{\text{DC\_TPT}} \cdot \tag{9}$$

Thus, the following effective area is derived as

$$S_{\text{eff\_LOOP}}\left(d \geq d_{\text{m}}\right) = 2 y_{\text{impact}} L_{\text{T}} = \left(a_2 + w - 2 L_{\text{DC\_TPT}}\right) L_{\text{T}} \cdot \tag{10}$$

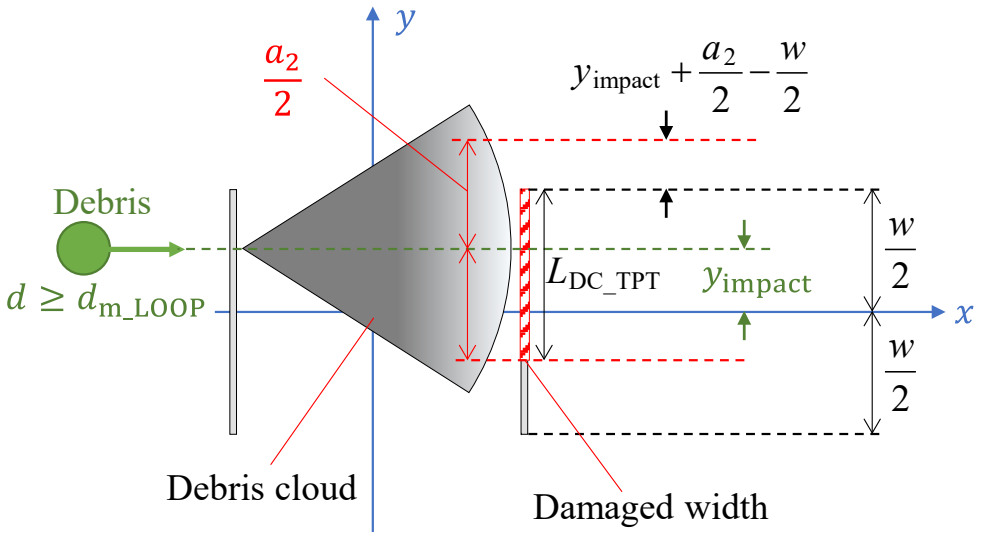


**Fig. 13.** Schematic of damage of tape tether for $d \geq d_{\text{m\_LOOP}}$.

### 3.4. Calculation Results of Rate of Severance

Table 3 lists the modeling assumptions established in Sections 2.2.3–2.2.4. The NASA Orbital Debris Engineering Model (ORDEM 2000) was used as the database of debris cumulative flux values [23]. The flux of 2013 at the 850 km altitude circular orbit at an inclination of 63° was used in this study [11]. Figure 14 shows the debris flux on the orbit (circular orbit, 850 km altitude, 63° inclination, 2013), which was obtained with ORDEM 3.0 [21]. Here, "local azimuth" is the angle measured in the local horizontal plane, from left to right, and "local elevation" is measured in a plane perpendicular to the local horizontal, from bottom to top. The majority of the flux lies between –5° and 5° in the local elevation angle. Figure 15 compares $R_{\text{LOOP}}$ and $R_{\text{FLT}}$. $R_{\text{LOOP}}$ is the rate of severance of the loop calculated with the modeling assumptions of the "LOOP" column in Table 3, and $R_{\text{FLT}}$ is the rate of severance of the flat-shaped tape tether calculated with the modeling assumptions of the "FLT" column in Table 3. Because $R_{\text{LOOP}}$ is greater than $R_{\text{FLT}}$, the tape tethers are easily severed when the loops appear. In addition, $R_{\text{LOOP}}$ is an upward convex curve against $r$, resulting from the upward convex curve of $a_2 / d$ against $r$ (Fig. 12).

**Table 3.** Modelling assumptions on calculation of rate of severance.

| | Tape tether (TPT) | | Solid cylindrical tether (SCT) |
|---|---|---|---|
| | Loop shaped part (LOOP) | Flat shaped part (FLT) | |
| Impact angle | $\theta = 0°$ | $\theta$ = 0–360° [11] | $\theta$ = 0–360° [20] |
| Criterion of severance | $L_{\text{DC\_TPT}} \equiv (1 - 1/\text{FoS})\, w$ | | $L_{\text{DC\_SCT}} = 0.3 D_{\text{T}}$<br>$D_{\text{T}}$: Diameter of a SCT [20] |
| Minimum diameter | $d_{\text{m\_LOOP}} \equiv L_{\text{DC\_TPT}} / f_{\text{LOOP}}$ | $d_{\text{m\_FLT}} = \frac{L_{\text{DC\_TPT}}}{0.45}\left(\frac{\cos\theta}{7.0}\right)^{0.65}$ [11] | $d_{\text{m\_SCT}} = \frac{1}{3} D_{\text{T}}$ [20] |
| Effective collision area | $\begin{cases} S_{\text{eff\_LOOP}} \\ = (a_2 + w - 2L_{\text{DC\_TPT}})\, L_{\text{T}} \\ a_2 = d \times f_{\text{LOOP}} \end{cases}$ | $S_{\text{eff\_FLT}} = (w\cos\theta + d - d_{\text{m\_FLT}})\, L_{\text{T}}$ [11] | $S_{\text{eff\_SCT}} = (0.7 D_{\text{T}} + d)\, L_{\text{T}}$ [20] |

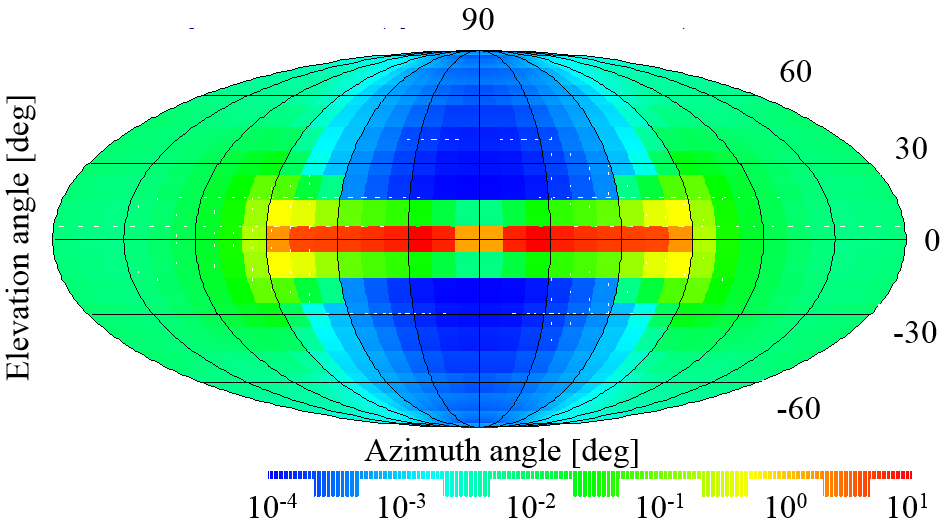


**Fig. 14.** Debris flux on the orbit used in the calculation (circular orbit, 850 km altitude, 63° inclination, 2013).

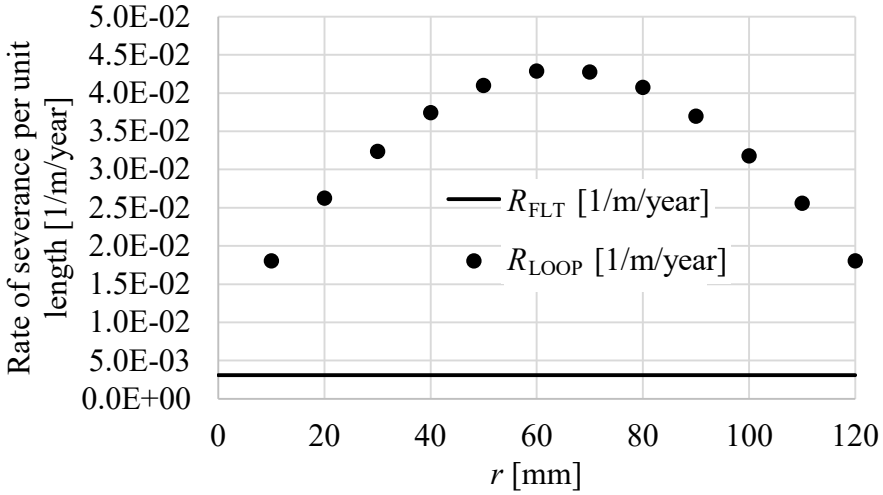


**Fig. 15.** Comparison of $R_{LOOP}$ and $R_{FLT}$.

$R_{TPT}$ is the rate of severance of the tape tether including the loop and the flat shape in the shape mixture ratio $\gamma$, and calculated with the modeling assumptions of the "LOOP" and "FLT" columns in Table 3. $R_{SCT}$ is the rate of severance of the conventional solid cylindrical tether calculated with the modeling assumptions of the "SCT" column in Table 3. Figure 16 compares $R_{TPT}$ under $\gamma = 0.002$ and $R_{SCT}$. The linear densities of the tape tether and the solid cylindrical tether are set to be the same. $R_{TPT}$ and $R_{FLT}$ show a small difference, and they are significantly smaller than $R_{SCT}$. Thus, when $\gamma$ is small, the tape tethers have a significant advantage even with the loops. Figure 17 compares $R_{TPT}$ under $\gamma = 0.1$ and $R_{SCT}$, where the linear densities of the tape tether and the solid cylindrical tether are set to be the same. The values of $R_{SCT}$ and $R_{FLT}$ are the same as those in Fig. 16. Because $R_{FLT}$ is smaller than $R_{SCT}$, tape tethers are useful when they maintain their ideal flat shape. However, $R_{TPT}$, which considers the influence of loops, is greater than $R_{SCT}$; in this case, there is little advantage for tape tethers.

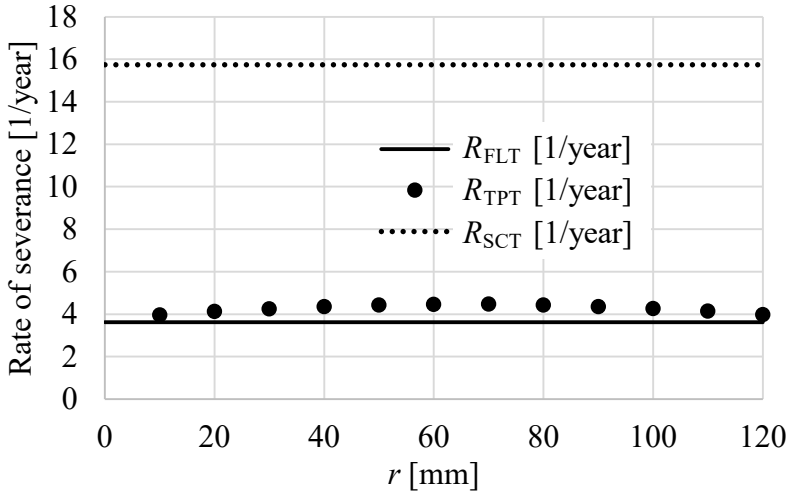


**Fig. 16.** Comparison at same linear density ( $\gamma = 0.002$).

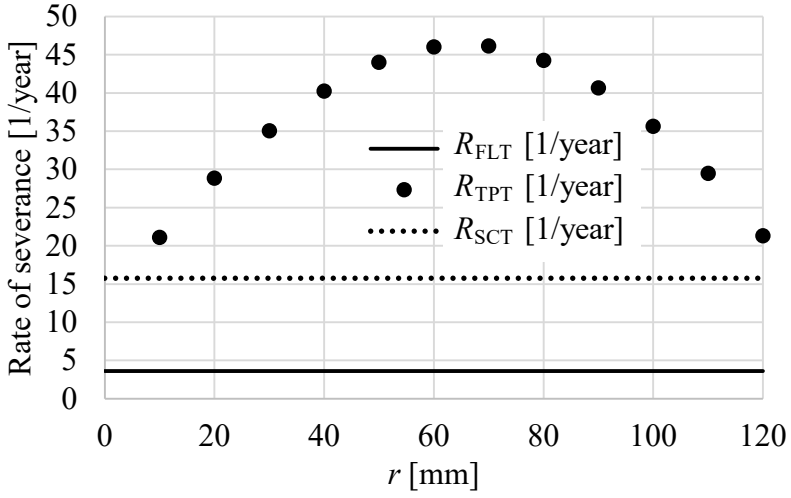


**Fig. 17.** Comparison at same linear density ( $\gamma = 0.1$).

## 4. Conclusions

The practicability of tape tethers was evaluated when they were twisted and transformed into a loop shape. In the HVI experiments, targets with a shape imitating a loop were impacted by the projectiles. The damage on the loops was analyzed by varying the loop radius. The damage size in the lateral direction was also measured. The changes in the size of the damage of the tape tethers depending on their shape were evaluated quantitatively by comparing the damaged length obtained from the HVI experiments with that from the previous studies assuming that the tape tethers are always flat.

Next, the rate of the severance of tape tethers was estimated when the tape tethers were twisted and transformed to the loop shape. The minimum diameter of the debris that may sever the tape tethers was derived from the results of the HVI experiments. The rate of severance was estimated based on this minimum diameter. The change in the rate of severance depending on their shape was evaluated quantitatively by comparing the rate of severance of looped tape tethers with that from the previous studies assuming that the tape tethers always maintain an ideal flat shape. In addition, the advantage of the tape tether was evaluated quantitatively by comparing the rate of severance with that of the conventional solid cylindrical tether.

When a few loops are generated (loop ratio = 0.002), the rate of severance of the tape tether is much lower than that of the conventional solid cylindrical tethers. Because of the assumption of $\theta = 0°$, the rate of severance of the tape tether is evaluated strictly on the safe side. Therefore, the tape tethers are more practical than the conventional solid cylindrical tethers when a few loops appear. In contrast, when 10% of the total length is in a looped configuration (loop ratio = 0.1), the tape tethers appear to be more easily severed than the conventional solid cylindrical tethers due to increased debris collisions. However, further investigation that includes all impact angles is required to adequately assess which type of tether is more susceptible to particle impacts under these conditions.

Finally, the loop part of a tape tether system was evaluated. This loop study will contribute to the success of tape tether missions by removing space debris, thus accelerating space development. Moreover, the tape tether evaluation presented in this paper can be applied to the design of gravity-gradient tapes and space elevators using thin and long tethers.

## Acknowledgements

The experiments were conducted at the HVI Facility (former name: The Space Plasma Laboratory) of Institute of Space and Astronautical Science (ISAS) of Japan Aerospace Exploration Agency (JAXA). The experiments were also supported by and conducted in collaboration with ISAS/JAXA and the Interdisciplinary Shock Wave Research Center of the Institute of Fluid Science at Tohoku University.

## References

[1] Liou JC, Johnson NL, Hill NM. Controlling the growth of future LEO debris populations with active debris removal. *Acta Astronaut* 2010;66:648–653. doi:10.1016/j.actaastro.2009.08.005.

[2] Liou JC. An active debris removal parametric study for LEO environment remediation. *Adv Space Res* 2011; 47:1865–1876. doi:10.1016/j.asr.2011.02.003.

[3] Mogi T, Kuwahara T, Uto H. Structural design of de-orbit mechanism demonstration cubesat FREEDOM. *Trans Japan Soc Aeronaut Space Sci, Aerosp Technol Japan* 2016;14:61–68. doi:10.2322/tastj.14.Pf_61.

[4] Sanmartin JR, Martinez-Sanchez M, Ahedo E. Bare wire anodes for electrodynamic tethers. *J Propuls Rocket* 1993;9:353–360. doi:10.2514/3.23629.

[5] Hayashida KB, Robinson JH. TSS tether cable meteoroid/orbital debris damage analysis. *NASA Tech Memo* 1993;3190: 1–23.

[6] Pardini C, Hanada T, Krisko PH, Anselmo L, Hirayama H. Are de-orbiting missions possible using electrodynamic tethers? Task review from the space debris perspective. *Acta Astronaut* 2007;60:916–929. doi:10.1016/j.actaastro.2006.11.001.

[7] Makihara K, Takahashi R. Survivability evaluation of electrodynamic tethers considering dynamic fracture in space-debris impact. *J Spacecr Rockets* 2016;53:209–216. doi:10.2514/1.A33328.

[8] Kawamoto S, Makida T, Sasaki F, Okawa Y, Nishida S. Precise numerical simulations of electrodynamic tethers for an active debris removal system. *Acta Astronaut* 2006;59:139–148. doi:10.1016/j.actaastro.2006.02.035.

[9] Makihara K, Matsumoto N. Survival probability of hollow cylindrical mesh tether under space debris impact. *J Spacecr Rockets* 2016;53:520–527. doi:10.2514/1.A33379.

[10] Francesconi A, Giacomuzzo C, Bettiol L, Lorenzini E. A new ballistic limit equation for thin tape tethers. *Acta Astronaut* 2016;129:325–334. doi:10.1016/j.actaastro.2016.09.023.

[11] Khan SB, Francesconi A, Giacomuzzo C, Lorenzini EC. Survivability to orbital debris of tape tethers for end-of-life spacecraft de-orbiting. *Aerosp Sci Technol* 2016;52:167–172. doi:10.1016/j.ast.2016.02.033.

[12] Makihara K, Kondo S. Structural evaluation for electrodynamic tape tethers against hypervelocity space debris impacts. *J Spacecr Rockets* 2018;55:462–72. doi:10.2514/1.A34023.

[13] Fujii HA, Watanabe T, Kojima H, Oyama K, Kusagaya T, Yamagiwa Y, Ohtsu H, Cho M, Sasaki S, Tanaka K, Williams J, Rubin B, Johnson CL, Khazanov G, Sanmartin JR, Lebreton JP, Heide EJ, Kruijff M, Pascal FD, Trivailo PM. Sounding rocket experiment of bare electrodynamic tether

system. *Acta Astronaut* 2009;64:313–324. doi:10.1016/j.actaastro.2008.07.006.
[14] Fujii HA, Watanabe T, Sahara H, Kojima H, Takehara S, Yamagiwa Y, Sasaki S, Abe T, Tanaka K, Oyama K, Johnson L, Khazanov GV, Sanmartin JR, Charro M, Kruijff M, Heide EJ, Rubin B, Quiros FJG, Trivailo PM, Williams P. Space demonstration of bare electrodynamic tape-tether technology on the sounding rocket S520-25. *AIAA Guidance Navig Control Conf* 2011:1–12. doi:10.2514/6.2011-6503.
[15] Chopin J, Kudrolli A. Helicoids, wrinkles, and loops in twisted ribbons. *Phys Review Lett* 2013;111:1–5. doi:10.1103/PhysRevLett.111.174302.
[16] Anderson CE, Trucano TG, Mullin SA. Debris cloud dynamics. *Int J Impact Eng* 1990;9:89–113. doi:10.1016/0734-743X(90)90024-P.
[17] Higashide M, Koura T, Akahoshi Y, Harada S. Debris cloud distributions at oblique impacts. *Int J Impact Eng* 2008;35:1573–1577. doi:10.1016/j.ijimpeng.2008.07.072.
[18] Mantri P, Mazzoleni AP, Padgett DA. Parametric study of deployment of tethered satellite systems. *J Spacecr Rockets* 2007;44(2):412–423. doi:10.2514/1.22955
[19] Jung W, Mazzoleni AP, Chung J. Dynamic analysis of a tethered satellite system with a moving mass. *Nonlinear Dyn* 2014;75(1–2):267–281. doi:10.1007/s11071-013-1064-8
[20] Hirayama H, Kim I, Hanada T. Survivability of tether throughout deorbiting. *Trans Japan Soc Aeronaut Space Sci, Aerosp Technol Japan* 2010;8:25–30. doi:10.2322/tastj.8.Pr_2_25.
[21] Orbital Debris Program Office. NASA orbital debris engineering model ORDEM 3.0 user's guide. *NASA Tech Pap* 2014;217370:1–63.
[22] Makihara M, Oki Y. Bayesian cloud extraction for assessment of space-debris impact using conditional entropy. *J Spacecr Rockets* 2017;54:1235–1245. doi:10.2514/1.A33856.
[23] Liou JC, Matney MJ, Anz-Meador PD, Kessler D, Jansen M, Theall JR. The new NASA orbital debris engineering model ORDEM2000. *NASA Tech Pap* 2002;210780:1–98.